Acta Crystallographica Section F
Structural Biology and Crystallization Communications
ISSN 1744-3091

Purification, crystallization and preliminary X-ray crystallographic analysis of squid heavy meromyosin

Elizabeth O'Neall-Hennessey,[a]‡ Ludmila Reshetnikova,[a]‡ V. S. Senthil Kumar,[a] Howard Robinson,[b] Andrew G. Szent-Györgyi[a] and Carolyn Cohen[a]*

[a]Rosenstiel Basic Medical Sciences Research Center, Brandeis University, 415 South Street, Waltham, MA 02454-9110, USA, and [b]Biology Department, Brookhaven National Laboratory, Upton, NY 11973-5000, USA

‡ These authors contributed equally to this work.

Correspondence e-mail: ccohen@brandeis.edu

Received 7 September 2012
Accepted 5 December 2012

All muscle-based movement is dependent upon carefully choreographed interactions between the two major muscle components, myosin and actin. Regulation of vertebrate smooth and molluscan muscle contraction is myosin based (both are in the myosin II class), and requires the double-headed form of myosin. Removal of Ca^{2+} from these muscles promotes a relatively compact conformation of the myosin dimer, which inhibits its interaction with actin. Although atomic structures of single myosin heads are available, the structure of any double-headed portion of myosin, including the ∼375 kDa heavy meromyosin (HMM), has only been visualized at low (∼20 Å) resolution by electron microscopy. Here, the growth of three-dimensional crystals of HMM with near-atomic resolution (up to ∼5 Å) and their X-ray diffraction are reported for the first time. These crystals were grown in off-state conditions, that is in the absence of Ca^{2+} and the presence of nucleotide analogs, using HMM from the funnel retractor muscle of squid. In addition to the crystallization conditions, the techniques used to isolate and purify this HMM are also described. Efforts at phasing and improving the resolution of the data in order to determine the structure are ongoing.

1. Introduction

Detailed structural information is essential to understand how myosin motors work and how they are regulated. The activated ('on'-state) myosin motor produces force by cycling between strong and weak actin-binding states. During the past 20 years, many states of the myosin head (referred to as S1) during the contractile cycle have been visualized at atomic resolution. This accomplishment has depended on investigations from a number of laboratories that have taken advantage of specialized features of myosins from different muscle types. Molluscan muscles have been the primary source of myosin used in this laboratory because they have allowed the visualization of an unmodified S1 (molecular mass of ∼130 kDa) containing a full-length lever arm, unlike non-molluscan myosins, which have required truncated or methylated constructs for crystallization (Dominguez *et al.*, 1998; Rayment *et al.*, 1993). Using scallop striated muscle, numerous weak actin-binding states of S1 have been visualized (Alamo *et al.*, 2008; Gourinath *et al.*, 2003; Himmel *et al.*, 2002; Houdusse *et al.*, 1999, 2000; Risal *et al.*, 2004; Woodhead *et al.*, 2005). In contrast, the ability to visualize strong actin-binding rigor-like states of the myosin motor, in the absence of actin, required different isoforms: first, that of nonmuscle myosin V by the Houdusse group (Coureux *et al.*, 2003) and subsequently squid fast funnel retractor muscle and scallop catch muscle myosin determined in this laboratory (Yang *et al.*, 2007).

Myosin is generally in a stable resting, or 'off', state. In vertebrate striated muscles, the tropomyosin–troponin complex on the thin filament regulates contractile activity. In vertebrate smooth muscle and in molluscan muscles, changes in the conformation of myosin itself control contraction (for a review, see Szent-Györgyi, 2007; see also Jung *et al.*, 2008; Jung & Craig, 2008). In contrast to the on-state, where a single S1 head is the minimal functional unit of the motor, a functional off-state of these regulated myosins requires a larger portion of the molecule. The two heads of the myosin dimer together

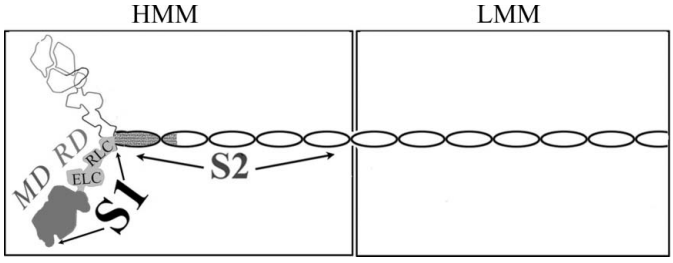

Figure 1
Schematic representation of the domains of myosin. Portions whose atomic structures have been determined are shaded in variations of gray.

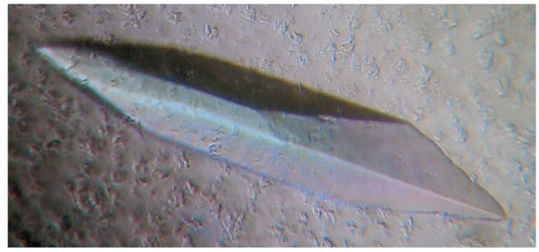

Figure 2
Crystal of squid heavy meromyosin (500 µm in length).

with (part of) its α-helical coiled-coil tail (molecular mass of ∼375 kDa for HMM; Fig. 1) is the minimal unit that is regulated (Cremo *et al.*, 1995; Kalabokis *et al.*, 1996; Trybus, 1994). This soluble dimer unit of minimally proteolyzed myosin retains the full sensitivity, activity and cooperativity of myosin without aggregating at low ionic strength (40 m*M*) owing to the removal of the filament-forming tail region.

Regulatory ions change the conformation of myosin from a generally compact off-state conformation, where the two heads contact each other asymmetrically and fold back towards the tail, to a relatively extended relationship between the tail and independently mobile heads. This change in shape has been determined by sedimentation studies of scallop HMM, where, in the presence of ADP or ATP analogs, calcium yields a slower sedimentation velocity compared with that in EGTA (Stafford *et al.*, 2001). The compact shape of the off-state of HMM, myosin and/or the thick filament from various species has also been viewed directly by electron microscopy (at a resolution of ∼20 Å) (Brito *et al.*, 2011; Burgess *et al.*, 2007; Jung *et al.*, 2008; Wendt *et al.*, 2001; Zhao *et al.*, 2009).

A high-resolution structure of double-headed myosin is nevertheless essential to understand fully how the off-state is achieved in regulated myosins. Crystallizing the far larger and fully sensitive and active HMM has been a long and painfully elusive pursuit. For example, despite many years of effort, we have been able to obtain only needles or fibril microcrystals from the bay scallop (*Argopecten irradiens*) HMM (unpublished work). It is indeed often difficult to crystallize such a large molecule, especially one that (for the vertebrate smooth muscle isoform) has been shown recently in solution to populate a mixture of disparate conformations, even in the absence of regulatory ions (Kast *et al.*, 2010; Vileno *et al.*, 2011). Fortunately, by switching to the funnel retractor muscle of squid (*Loligo pealei*), we have been able to obtain single crystals of HMM for the first time. We report here the isolation, purification and crystallization of this HMM, as well as the X-ray diffraction results that have been obtained.

2. Materials and methods

2.1. Protein isolation and digestion

Squid (*Loligo pealei*, common name longfin inshore squid) were obtained from the Marine Biological Laboratory in Woods Hole, Massachusetts, USA. The funnel retractor muscle was harvested and myosin was prepared as described by Stafford *et al.* (1979) with slightly longer spin times and higher *g*-force owing to looser pellets with the squid muscle. All protein work was performed on ice unless otherwise specified. Protein purity was analyzed at all steps by SDS–PAGE gels (Laemmli, 1970) stained with Coomassie Brilliant Blue R250.

Squid myosin was digested to HMM as described by Stafford *et al.* (2001) with the following modifications. The digestion time was 3 min. Saturated ammonium sulfate solution (SAS; pH 6.7) was added to the dialyzed HMM to 48%, then centrifuged. The supernatant was filtered, its volume measured and it was then precipitated with 55% SAS. The pellet was dissolved in a small volume of standard HMM buffer (80 m*M* NaCl, 20 m*M* MOPS pH 7, 3 m*M* NaN_3, 2 m*M* $MgCl_2$, 0.2 m*M* EGTA, 0.2 m*M* K-ADP, 0.5 m*M* DTT, 0.5 µg ml^{-1} leupeptin) and stored on ice for 3–5 d prior to continuing.

2.2. Protein purification

The 55% SAS HMM pellet was dialyzed against 100-fold volume of standard HMM buffer for 4 h, then transferred to a 40-fold to 50-fold volume of start buffer (500 m*M* KCl, 20 m*M* potassium phosphate, 3 m*M* NaN_3, 0.5 m*M* $MgCl_2$, 0.1 m*M* EGTA, 0.5 m*M* DTT, 0.2 m*M* K-ADP, 0.5 µg ml^{-1} leupeptin) pH 6.8, and dialyzed overnight. The dialyzed HMM was applied onto a hydroxylapatite (HA) column (Calbiochem, Fast Flow; 1 g HA per 6.7 mg HMM) equilibrated in start buffer and rinsed with 2–3 column volumes. The column was washed with potassium phosphate buffers of increasing molarity and pH (with all other buffer components remaining constant). HMM of varied purity eluted with each buffer. All HMMs were precipitated with SAS as described previously (48% followed by 60%) and dialyzed *versus* standard HMM buffer (several changes) to remove ammonium sulfate. Dialyzed samples were clarified with a 30 min spin at 100 000*g*. The 60% pellet samples were used hereafter. Sample sensitivity and Ca^{2+}-activated activity were determined by the coupled assay method (Kalabokis & Szent-Györgyi, 1997).

The HA-purified HMM (both 50 and 75 m*M* potassium phosphate) was run over a Superdex 200 column (Pharmacia GE 1×30 cm) at room temperature in 40 m*M* sodium malonate pH 7, 20 m*M* 4-(*N*-morpholino)butanesulfonic acid (MOBS) pH 7.5, 3 m*M* NaN_3, 2.5 m*M* $MgCl_2$, 0.2 m*M* EGTA, 0.5 m*M* tris(2-carboxyethyl)phosphine hydrochloride (TCEP), 0.5 µg ml^{-1} leupeptin, 50 µ*M* adenosine 5′-(β,γ-imido)triphosphate tetralithium salt hydrate (AMPPNP). Purified fractions were combined, AMPPNP was increased to 0.2 m*M* and the samples were concentrated (Centricon/Microcon spin units). AMPPNP was then increased to 2 m*M* and the final samples were clarified with a 30 min spin at 80 000*g*. Protein concentration was determined by the Bradford method (specifically, Bio-Rad Protein Assay), and ATPase sensitivity and activity were determined. Concentrations varied from 3 to 4 mg ml^{-1}; sensitivity was 90+%; activity varied from 0.3 to 0.45 mol^{-1} s^{-1}.

2.3. Crystallization experiments

Squid HMM-AMPPNP crystals were grown by the sitting-drop vapor-diffusion method at 277 K (using Hampton Research microbridges). Sitting drops were prepared by mixing 2.5 µl precipitant

Table 1
Data-collection statistics..

Values in parentheses are for the highest-resolution shell.

No. of crystals	1
Beamline	A1, Cornell High Energy Synchrotron Source
Wavelength	0.977
Detector	Quantum 210 CCD detector
Crystal–detector distance (mm)	480
Rotation range per image (°)	1
Total rotation range (°)	360
Exposure time per image (s)	60
Resolution range (A)	50–5.07 (5.16–5.07)
Space group†	$P2_12_12_1$
Unit-cell parameters (A,°)	a = 143.9, b = 167.6, c = 531.0, $\alpha = \beta = \gamma$ = 90
Mosaicity (°)	0.300
Total no. of reflections	259264
Unique reflections	44222
Multiplicity	3.8 (3.7)
$\langle I/\sigma(I)\rangle$	14.9 (1.7)
Completeness (%)	83.7 (46.3)
$R_{\rm merge}$‡ (%)	0.202 (0.412)
Overall B factor from Wilson plot (Å^2)	247.7
Optical resolution	3.89

† Space-group assignment is based on the low metric tensor distortion index for primitive orthorhombic determined by *HKL*-2000 and the presence of h = odd, k = odd and l = odd systematic absences in the $h00$, $0k0$ and $00l$ directions, respectively. We do not yet know the exact number of molecules in the asymmetric unit. Values of 1, 2, 3 and 4 would yield solvent contents of 86.4, 72.8, 59.3 and 45.7%, respectively. ‡ $R_{\rm merge} = \sum_{hkl}\sum_i |I_i(hkl) - \langle I(hkl)\rangle|/\sum_{hkl}\sum_i I_i(hkl)$.

solution [10%(*w*/*v*) polyethylene glycol 20000 (PEG 20K), 4% ethylene glycol (EG), 20 m*M* 2-aminoethane sulfonic acid (taurine), 20 m*M* MOBS pH 8.0, 0.5 m*M* TCEP, 0.2 m*M* EGTA, 2 m*M* NaN_3] with 7.5 µl protein solution. Some drops were set up with a final molarity of 0.14 m*M* chromium(III) acetylacetonate [$Cr(acac)_3$] (Acros Organics) in the protein and/or precipitant solution. The drops were equilibrated against 1 ml reservoir solution (5% PEG 20 K, 2% EG, 40 m*M* MOBS pH 8.0, 60 m*M* sodium malonate, 10 m*M* taurine, 2 m*M* NaN_3) for 3–4 weeks. Crystals appeared after 2 weeks and grew to dimensions of up to ∼0.5 × 0.1 × 0.05 mm (Fig. 2).

To prepare crystals for freezing, the concentration of cryoprotectant PEG 400 in the drop was increased slowly up to 5, 10, 15 and then 20%, with corresponding supplements of PEG 20 K up to 10–12% and EG at not more than 3%. Each crystal was picked up in a loop and frozen by immersion in liquid nitrogen, where it was stored until diffraction experiments.

2.4. X-ray data collection and analysis

Well over 5000 crystals were screened, primarily at the Brookhaven National Laboratory (BNL) and Cornell High Electron Synchrotron Source (CHESS) synchrotrons, with the best data set obtained at 100 K at CHESS using beamline A1 (λ = 0.939 Å). Diffraction data were processed using *HKL*-2000 (Otwinowski & Minor, 1997). X-ray data were collected from a squid HMM-AMPPNP chromium crystal. Data-processing statistics shown in Table 1 are from a single crystal which diffracted to 5.07 Å resolution, with a complete data set to 7 Å resolution (Fig. 3 and Table 1).

3. Results and discussion

Regulated myosins are in the off-state in the absence of calcium and the presence of ATP. This off-state is not specific to ATP, since numerous ATP analogs have yielded a similar post-rigor structure in S1 (Himmel *et al.*, 2002). Certain analogs, however, may be more representative than others of ATP bound in a physiological environment. Sedimentation rates of scallop HMM with AMPPNP are the most similar to those observed with ATP with or without Ca^{2+} (Stafford *et al.*, 2001). It made sense to utilize this slowly hydrolyzing ATP analog for our crystallization experiments, since HMM remains fully functional (normal sensitivity and activity) in the presence of non-cross-linked AMPPNP, enabling a mimicking of an *in vivo* ATP-HMM. To maintain the sample in its off-state, no Ca^{2+} was ever introduced and at least 0.2 m*M* EGTA was present.

Our digestion of squid myosin produced one major band of HMM (along with a non-removable ∼70 kDa fragment; the C-terminus of the HMM was not determined). This differs from the two HMMs obtained from digestion of scallop myosin (owing to alternative digestion sites in the tail) and on SDS gels the heavy-chain portion runs in between the two heavy chains observed in scallop HMM. This initial crude squid HMM is very stable when stored as the 55% SAS

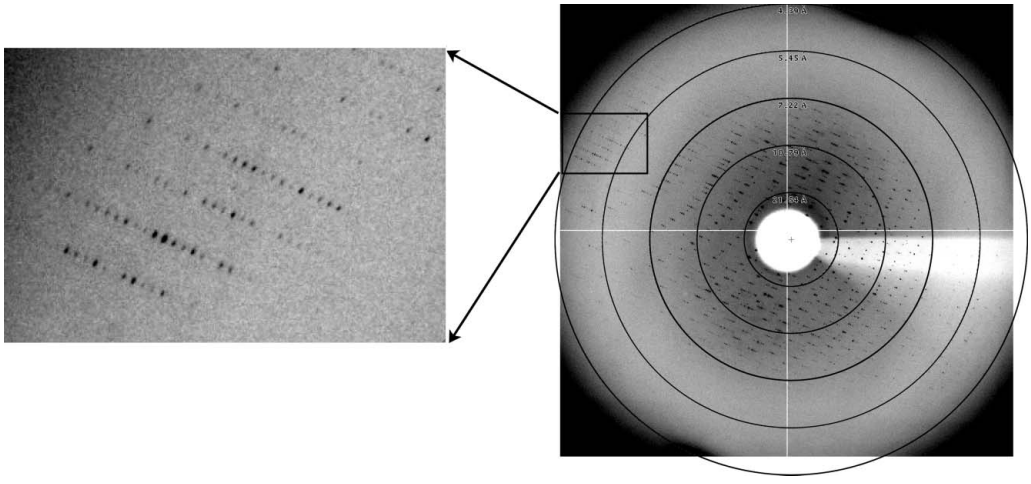

Figure 3
X-ray diffraction image of squid HMM crystal. The five resolution rings in the right image are at 21.54, 10.79, 7.22, 5.45 and 4.39 Å; the latter two pass through the boxed region, which is magnified in the left image. Note that the diffraction is anisotropic, *i.e.* diffraction is observed past 4.4 Å resolution in some directions but to only ∼7 Å resolution in other directions, and a second minor lattice is seen at low resolution. (These factors may account in part for the relatively high $R_{\rm merge}$ given in Table 1.)

pellet, remaining fully sensitive and active for weeks, with no degradation, thus offering a safe 'stopping' point for the protein prior to continuing with the purification. The 50 m*M* potassium phosphate portion from the HA column contained the most S1 and had the lowest overall yield of HMM, but it also contained the least amount of higher-molecular-weight contamination. Following a sizing-column run, this sample exhibited the greatest ability to crystallize. The sizing-column-purified 75 m*M* potassium phosphate HMM also crystallized well. The final purified HMM is stable for at least 1 month. Since no sequencing was performed on our trypsin-derived HMM samples, it is unknown whether there are multiple isoforms present (Matulef *et al.*, 1998; Shaffer & Kier, 2012) in the initial digestion product, nor whether subsequent purification separates them.

Although crystals were obtained from flash-frozen/thawed HMM, use of fresh, non-frozen material increased the size of the crystals (as well as the reproducibility). This result shows a marked change from results with S1, where previously frozen material produced crystals equal to fresh material. The first HMM-AMPPNP crystals (elongated hexagonal shaped) grew to 0.25 × 0.05 × 0.03 mm and diffracted up to 10 Å resolution. Optimization of crystal conditions resulted in larger crystals (0.5 × 0.1 × 0.05 mm) and consisted of using sitting drops (10 µl), MOBS buffer pH 8, TCEP, adding 10 m*M* taurine, a naturally produced osmolyte in squid (Cohen, 1958) that can stabilize protein structure (Bolen, 2004; Jeruzalmi & Steitz, 1997), and exchanging NaCl for sodium malonate. Freezing with PEG 400, in combination with these optimized conditions, improved crystal diffraction to 8 Å resolution. With regard to the cryocooling procedure harming the crystals, both non-frozen and frozen (then annealed) crystals were checked for diffraction at room temperature; neither diffracted, so this gives no definitive answer. Given the challenge of freezing the HMM crystals, many dehydrating reagents were tested, but none gave positive results. Numerous reagents, additives and detergents not included in any kits were also explored, such as raffinose, ectoine, aspartame, sucralose, melizitose, carnitine, carnosine, ionic liquids (IOLITECs kit), nanospheres, as well as the compound trifluoperazine (TFP; it has been shown that micromolar concentrations of TFP bind to scallop myosin, locking it in a conformation resembling the off-state; Patel *et al.*, 2000). There was no improvement, however, in the diffraction quality of the crystals grown in the presence of any of these additives and many crystals did not diffract at all. There was also no success with numerous metals (both gold and $SmCl_3$ yielded only small poor-quality crystals and crystals grown in the presence of iridium diffracted very poorly). Only with the addition of $Cr(acac)_3$ (0.14 m*M* in the crystallization drop), along with the optimized conditions discussed above, was an improvement in diffraction obtained, as well as increasing the number of crystals giving any diffraction at all. It should be noted that the presence of chromium in the crystal was not verified by fluorescence. The probability of having an HMM crystal that diffracted was extremely low, so several sources were used for screening. A nearly complete data set to 8 Å resolution was achieved at BNL. A crystal screened at CHESS showed diffraction past 4.4 Å resolution in some directions (Fig. 3). From this crystal, a nearly complete data set was obtained to 7 Å resolution and a partial data set to 5.07 Å resolution (Table 1).

In addition to continued efforts to improve the quality, resolution and reproducibility of the X-ray diffraction, efforts are also under way to phase the data. Heavy-atom-derivatized crystals that have diffracted include those with 5-amino-2,4,6-triiodoisophthalic acid (I3C; 9–10 Å resolution) and a tantalum bromide cluster (10–12 Å resolution) and we are currently working on obtaining data sets. No molecular-replacement solution using electron-microscopy-derived models (Wendt *et al.*, 2001; Zhong Huang & Kenneth Taylor, personal communication) has yet been found.

Sequence database references: squid regulatory light chain: P08052 (*Todarodes pacificus*); squid essential light chain: P05945 (*Todarodes pacificus*); squid myosin heavy chain: O44934 (*Loligo pealei*; also referenced as *Doryteuthis pealeii*). Conflicts with O44934: Glu238 to Lys; Val744 to Ala; Ser864 to Arg; Ala1495 to Glu; His1531 to Arg; Gly1548 to Ala (changes submitted in 2009).

We thank Jerry Brown for helpful discussions, his attempts to phase the current data by molecular replacement and for his work on the manuscript. We also thank Karen Allen for suggesting the use of chromium(III) acetylacetonate to improve diffraction, colleagues and the staff of the BNL and CHESS synchrotrons (in particular Marian Szebenyi and Irina Kriksunov) for assistance with and/or the carrying out of data collection and former members of the Cohen laboratory for their help with screening the first HMM crystals obtained. This work is supported by NIH/NIAMS grant No. AR017346 to CC. Its contents are solely the responsibility of the authors and do not necessarily represent the official views of the NIAMS or NIH.

References

Alamo, L., Wriggers, W., Pinto, A., Bártoli, F., Salazar, L., Zhao, F. Q., Craig, R. & Padrón, R. (2008). *J. Mol. Biol.* **384**, 780–797.
Bolen, D. W. (2004). *Methods*, **34**, 312–322.
Brito, R., Alamo, L., Lundberg, U., Guerrero, J. R., Pinto, A., Sulbarán, G., Gawinowicz, M. A., Craig, R. & Padrón, R. (2011). *J. Mol. Biol.* **414**, 44–61.
Burgess, S. A., Yu, S., Walker, M. L., Hawkins, R. J., Chalovich, J. M. & Knight, P. J. (2007). *J. Mol. Biol.* **372**, 1165–1178.
Cohen, C. (1958). *J. Biophys. Biochem. Cytol.* **4**, 489–490.
Coureux, P. D., Wells, A. L., Ménétrey, J., Yengo, C. M., Morris, C. A., Sweeney, H. L. & Houdusse, A. (2003). *Nature (London)*, **425**, 419–423.
Cremo, C. R., Sellers, J. R. & Facemyer, K. C. (1995). *J. Biol. Chem.* **270**, 2171–2175.
Dominguez, R., Freyzon, Y., Trybus, K. M. & Cohen, C. (1998). *Cell*, **94**, 559–571.
Gourinath, S., Himmel, D. M., Brown, J. H., Reshetnikova, L., Szent-Györgyi, A. G. & Cohen, C. (2003). *Structure*, **11**, 1621–1627.
Himmel, D. M., Gourinath, S., Reshetnikova, L., Shen, Y., Szent-Györgyi, A. G. & Cohen, C. (2002). *Proc. Natl Acad. Sci. USA*, **99**, 12645–12650.
Houdusse, A., Kalabokis, V. N., Himmel, D., Szent-Györgyi, A. G. & Cohen, C. (1999). *Cell*, **97**, 459–470.
Houdusse, A., Szent-Gyorgyi, A. G. & Cohen, C. (2000). *Proc. Natl Acad. Sci. USA*, **97**, 11238–11243.
Jeruzalmi, D. & Steitz, T. A. (1997). *J. Mol. Biol.* **274**, 748–756.
Jung, H. S., Burgess, S. A., Billington, N., Colegrave, M., Patel, H., Chalovich, J. M., Chantler, P. D. & Knight, P. J. (2008). *Proc. Natl Acad. Sci. USA*, **105**, 6022–6026.
Jung, H. S. & Craig, R. (2008). *J. Mol. Biol.* **383**, 512–519.
Kalabokis, V. N. & Szent-Györgyi, A. G. (1997). *Biochemistry*, **36**, 15834–15840.
Kalabokis, V. N., Vibert, P., York, M. L. & Szent-Györgyi, A. G. (1996). *J. Biol. Chem.* **271**, 26779–26782.
Kast, D., Espinoza-Fonseca, L. M., Yi, C. & Thomas, D. D. (2010). *Proc. Natl Acad. Sci. USA*, **107**, 8207–8212.
Laemmli, U. K. (1970). *Nature (London)*, **227**, 680–685.
Matulef, K., Sirokmán, K., Perreault-Micale, C. L. & Szent-Györgyi, A. G. (1998). *J. Muscle Res. Cell Motil.* **19**, 705–712.
Otwinowski, Z. & Minor, W. (1997). *Methods Enzymol.* **276**, 307–326.
Patel, H., Margossian, S. S. & Chantler, P. D. (2000). *J. Biol. Chem.* **275**, 4880–4888.
Rayment, I., Rypniewski, W. R., Schmidt-Bäse, K., Smith, R., Tomchick, D. R., Benning, M. M., Winkelmann, D. A., Wesenberg, G. & Holden, H. M. (1993). *Science*, **261**, 50–58.
Risal, D., Gourinath, S., Himmel, D. M., Szent-Györgyi, A. G. & Cohen, C. (2004). *Proc. Natl Acad. Sci. USA*, **101**, 8930–8935.
Shaffer, J. F. & Kier, W. M. (2012). *J. Exp. Biol.* **215**, 239–246.

Stafford, W. F., Jacobsen, M. P., Woodhead, J., Craig, R., O'Neall-Hennessey, E. & Szent-Györgyi, A. G. (2001). *J. Mol. Biol.* **307**, 137–147.
Stafford, W. F. III, Szentkiralyi, E. M. & Szent-Györgyi, A. G. (1979). *Biochemistry*, **18**, 5273–5280.
Szent-Györgyi, A. G. (2007). *Adv. Exp. Med. Biol.* **592**, 253–264.
Trybus, K. M. (1994). *J. Biol. Chem.* **269**, 20819–20822.
Vileno, B., Chamoun, J., Liang, H., Brewer, P., Haldeman, B. D., Facemyer, K. C., Salzameda, B., Song, L., Li, H.-C., Cremo, C. R. & Fajer, P. G. (2011). *Proc. Natl Acad. Sci. USA*, **108**, 8218–8223.
Wendt, T., Taylor, D., Trybus, K. M. & Taylor, K. (2001). *Proc. Natl Acad. Sci. USA*, **98**, 4361–4366.
Woodhead, J. L., Zhao, F.-Q., Craig, R., Egelman, E. H., Alamo, L. & Padrón, R. (2005). *Nature (London)*, **436**, 1195–1199.
Yang, Y., Gourinath, S., Kovács, M., Nyitray, L., Reutzel, R., Himmel, D. M., O'Neall-Hennessey, E., Reshetnikova, L., Szent-Györgyi, A. G., Brown, J. H. & Cohen, C. (2007). *Structure*, **15**, 553–564.
Zhao, F.-Q., Craig, R. & Woodhead, J. L. (2009). *J. Mol. Biol.* **385**, 423–431.